═══════════════ **MAGNETISM** ═══════════════

Mössbauer Investigation of Temperature Transformations in Bacterial Ferrihydrite

S. V. Stolyar[a, b], **O. A. Bayukov**[a, b], **V. P. Ladygina**[c], **R. S. Iskhakov**[a, b], **L. A. Ishchenko**[a, b],
V. Yu. Yakovchuk[a, b], **K. G. Dobretsov**[d], **A. I. Pozdnyakov**[b], and **O. E. Piksina**[a]

[a] *Siberian Federal University, Svobodnyi pr. 79, Krasnoyarsk, 660041 Russia*

[b] *Kirensky Institute of Physics, Siberian Branch, Russian Academy of Sciences,*
Akademgorodok 50, Krasnoyarsk, 660036 Russia

* e-mail: rauf@iph.krasn.ru

[c] *International Research Center for Extreme States of the Organism, Presidium of Krasnoyarsk Scientific Center,*
Siberian Branch, Russian Academy of Sciences, Akademgorodok 50, Krasnoyarsk, 660036 Russia

[d] *Railway Clinical Hospital at the Krasnoyarsk station, Joint Stock Company "Russian Railways" (RZhD),*
pr. Mira 154, Krasnoyarsk, 660021 Russia

Received February 24, 2010; in final form, June 15, 2010

Abstract—Ferrihydrite nanoparticles formed as a result of the microorganism activity have been studied using Mössbauer spectroscopy, X-ray powder diffraction analysis, and X-ray fluorescence analysis. Three positions of trivalent iron with nonoverlapping ranges of quadrupole splittings have been revealed in bacterial ferrihydrite: QS{$Fe^{3+}(1)$} = 0.49–0.83 mm/s, QS{$Fe^{3+}(2)$} = 0.84–1.10 mm/s, and QS{$Fe^{3+}(3)$} = 1.25–1.73 mm/s. It has been experimentally demonstrated that the $Fe^{3+}(3)$ positions are the centers of nucleation of the hematite phase in the course of heat treatment.

1. INTRODUCTION

At present, considerable attention has been focused on the study of magnetic nanoparticles due to their unique physical characteristics and the wide spectrum of their possible applications [1]. In the vast majority of cases, the known technologies for synthesizing magnetic nanoparticles are based on physical and physicochemical methods used for processing initial materials (reagents and substances). The regularities of the synthesis of particles in cells of animals, plants, and microorganisms are radically different. This circumstance suggests that biogenic nanocrystals can have specific or unique characteristics that can be valuable for practical application in the preparation of various nanomaterials. Nowadays, ferrihydrite (which is a mineral core of the ferritin protein) has been produced in small amounts as a reagent for scientific investigations [2].

Ferrihydrite $Fe_2O_3 \cdot nH_2O$ belongs to antiferromagnets with the magnetic ordering temperature above room temperature (T_N = 340 K). The magnetic moments of the Fe^{3+} ions located on the particle surface are not compensated and form a "parasitic" net magnetic moment of an individual particle. The orientation diffusion of the magnetic moment of a nanoparticle under the action of a thermal fluctuation field comparable to the magnetic anisotropy field is responsible for the superparamagnetism of ferrihydrite particles [3]. The crystal lattice of ferrihydrite under external actions transforms into stoichiometric compounds [4].

In ferrihydrite (and defect hydroxides), two types of anion packings are mixed. During the formation of an element of the cubic packing in which anion planes are arranged in the sequence *ABCABC*, the Fe^{3+} ions are in an octahedral environment and form two-layer iron Fe(2): two neighboring layers of octahedra are occupied by iron. During the formation of an element of the hexagonal packing in which anion planes are arranged in the sequence *ABAB* (*ACAC*), there arises one-layer iron Fe(1): one layer of octahedra occupied by iron and one layer of empty octahedra. In an arbitrary alternation of sequences of cubic and hexagonal layers, which depends on the synthesis conditions, the ratio between the occupancies of the Fe(1) and Fe(2) positions can be arbitrary; most frequently, the Fe(1) and Fe(2) positions are occupied in a ratio of 1 : 2. For "perfect" ferrihydrites, two limiting cases of the crystal structures are distinguished: the magnetic-like (cubic) structure 2*LFh* with the parameter *a* = 8.40 Å and the hexagonal structure 6*LFh* with the parameters *a* = 5.08 Å and *c* = 9.40 Å [5].

In our earlier work [6], we investigated the ferrihydrite synthesized by *Klebsiella oxytoca* bacteria with the use of Mössbauer spectroscopy and revealed that the structure contains up to four nonequivalent positions of iron ions with the same values of isomer chem-

ical shifts and different quadrupole splittings $QS(Fe(2)) \sim 0.5$ mm/s and $QS(Fe(1)) \sim 1.0$ mm/s, as well as the positions with a higher degree of distortion characterized by $QS(Fe) \sim 1.5-1.8$ mm/s. It was established that the occupancies of the positions depend on the time and conditions of cultivation of microorganisms (equal occupancies of the Fe(1) and Fe(2) positions were revealed for the first time). The factor responsible for the appearance of two nonequivalent positions in ferrihydrite is the formation of double and single layers of iron ions, which are separated by empty coordination octahedra. The Fe^{3+} ions of the double layers are surrounded by weakly distorted ligand octahedra, and the iron ions of the single layers are surrounded by more strongly distorted octahedra. The nature of the formation of strongly distorted positions of Fe ions in ferrihydrite nanoparticles remained unclear. In this work, we present the results of investigations of the transformation of the crystal structure of ferrihydrite nanoparticles synthesized by microorganisms in the course of heat treatment. The aim of our work is to reveal the nature of strongly distorted positions of Fe ions and to determine the phase composition of the nanoparticles formed as a result of thermal annealing.

2. EXPERIMENTAL PROCEDURE AND RESULTS

Microorganisms were cultivated for two weeks after inoculation into a liquid culture medium [6]. The prepared biomass was centrifuged and dried at a temperature of 40°C. Thermal annealing of samples was performed in a muffle furnace at temperatures of 300–700°C for 7 h. The chemical composition was determined by X-ray fluorescence analysis, and the phase composition was determined by X-ray powder diffraction analysis ($\lambda = 1.54178$ Å). The Mössbauer mea-

Table 1. Contents of chemical elements in bacterial ferrihydrite

Element	$T = 20°C$	$T = 300°C$	$T = 700°C$
O	60.5343	54.1077	48.148
C	16.5057	11.1661	5.6675
P	8.4520	12.0230	16.4718
Fe	9.198	14.3076	17.666
Ca	2.9274	4.4187	6.9768
K	1.6764	2.6153	4.1485
Cl	0.3269	0.6095	–
Other elements	0.3793	0.7521	0.9214

surements were carried out using a $Co^{57}(Cr)$ source with a line width at half height of 0.24 mm/s for a sodium nitroprusside powder absorber. The thickness of the samples under investigation was equal to 5–10 mg/cm^2 according to the natural iron content for which the intensities of spectral lines are linearly related to the iron content in the phase.

Table 1 presents the results of X-ray fluorescence analysis. The change in the chemical composition of the analyzed powders is caused by the presence of the organic component, which burns out as a result of the heat treatment.

The X-ray diffraction patterns of the initial sample and the sample annealed at $T = 300°C$ exhibited a broad line that is typical of an amorphous state and centered at $2\theta \approx 30°$. Figure 1 shows the X-ray diffraction pattern of the sample annealed at $T = 500°C$. The revealed reflections indicate the formation of the hematite phase α-Fe_2O_3. At $T = 700°C$, the crystallization took place. Figure 2 shows the X-ray diffraction

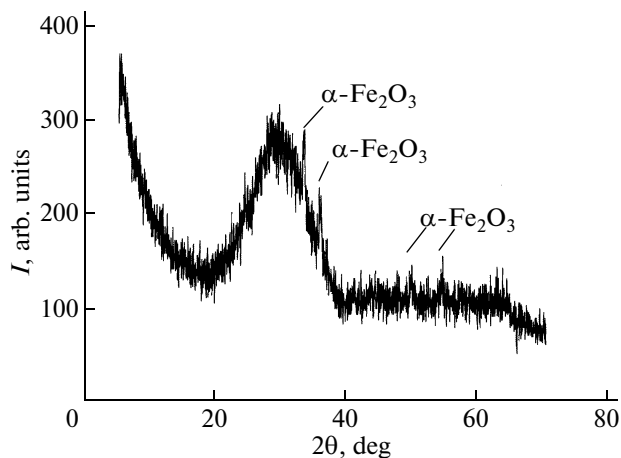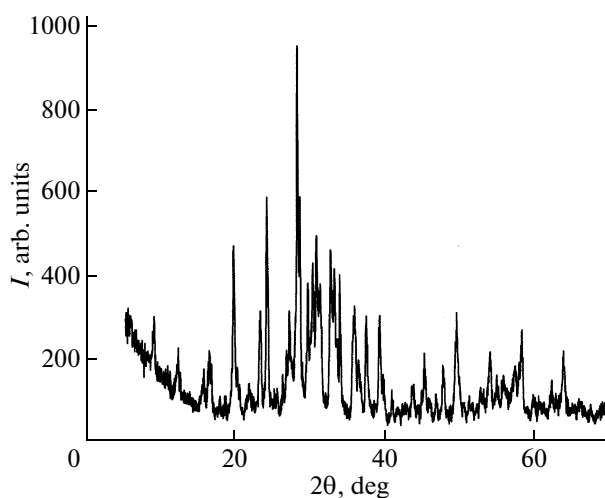**Fig. 1.** Diffraction pattern of the sample annealed at 500°C.

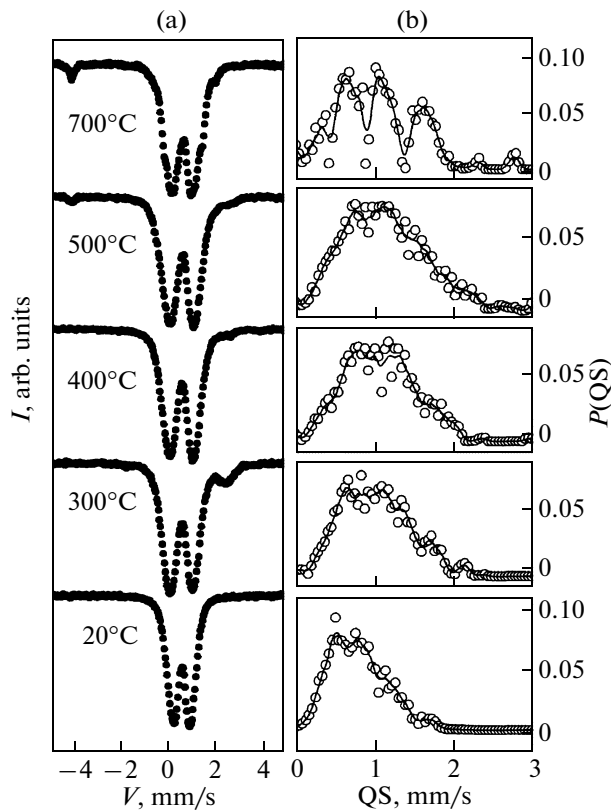**Fig. 2.** Diffraction pattern of the sample annealed at 700°C.

(a) (b)

Fig. 3. (a) Mössbauer spectra and (b) probabilities of the quadrupole splitting of the dried biomass annealed at different temperatures.

pattern of the sample annealed at $T = 700°C$. In addition to the reflections of α-Fe_2O_3, this X-ray diffraction pattern is characterized by a set of reflections of unidentified crystal phases.

The Mössbauer spectra of the initial and heat-treated samples (Fig. 3a) represent a sum of several quadrupole doublets and a Zeeman sextet. The spectra were identified in two stages. At the first stage, the experimental spectra were used to determine the probability distributions of quadrupole splittings by fitting a common isomer chemical shift and the probability distributions of hyperfine fields by fitting common isomer and quadrupole shifts. The results obtained are presented in Fig. 3b.

The maxima and specific features in the obtained dependences of the probabilities suggest the presence of possible nonequivalent positions and states of iron ions in the material under investigation. Since the probabilities were determined using one isomer chemical shift common to a group of doublets, a part of specific features in the dependences obtained can appear to be false. The observed specific features were used for constructing a model spectrum. At the second stage, the model spectrum was fitted to the experimental spectrum by varying all parameters of the hyperfine structure. In the course of fitting, the components of

false positions tend to zero. In addition, according to crystallographic considerations that will become clear in the following discussion, we restricted ourselves to three clear nonequivalent positions. The results of the identification of the spectra are summarized in Table 2.

The data presented in Table 2 indicate that iron is in three states: Fe(1), Fe(2), and Fe(3); in this case, regardless of the annealing temperature, the quadrupole splittings for three positions of trivalent iron of bacterial ferrihydrite take on values in quite specific nonoverlapping ranges, namely, $QS\{Fe^{3+}(2)\} = 0.84$–1.10 mm/s, $QS\{Fe^{3+}(1)\} = 0.49$–0.83 mm/s, and $QS\{Fe^{3+}(3)\} = 1.25$–1.73 mm/s. Therefore, the values of the quadrupole splittings can serve as indications that iron ions belong to a particular position. After annealing at 300°C, there appears bivalent iron ions with a characteristic isomer shift of ~1 mm/s. All three positions of Fe ions found for the as-prepared samples are characterized by reduction, which is indicated by the number of revealed positions of Fe^{2+} ions and the values of the quadrupole splittings: $QS\{Fe^{2+}(1)\} = 2.32$–2.68 mm/s, $QS\{Fe^{2+}(2)\} = 1.60$–2.15 mm/s, and $QS\{Fe^{2+}(3)\} = 2.80$–3.09 mm/s. The process of reduction $Fe^{3+} \longrightarrow Fe^{2+}$ is caused by the presence of carbon. Further annealing led to the oxidation processes. The Zeeman splitting is observed for the sample annealed at 700°C. The phase characterized by the sextet at room temperature is the hematite phase α-Fe_2O_3 with the typical hyperfine-structure parameters: $IS = 0.367$ mm/s, $H = 507$ kOe, and $QS = -0.42$ mm/s.

3. DISCUSSION OF THE RESULTS

Neutron diffraction [5] and X-ray diffraction [4] investigations demonstrated that ferrihydrite consists of double and single iron layers alternating along the c axis. All iron atoms are located in coordination ligand octahedra. The layers of octahedra occupied by iron are separated by layers of empty octahedra. In the single layer, the octahedra of the neighboring iron atoms are shared by edges. In the double layer, the octahedra of iron are also shared by edges both along and across the axis. However, the octahedra in empty layers and occupied octahedra in both single and double layers are shared by faces. This layer-by-layer distribution of iron leads to a relatively small distortion of octahedra in double layers (these positions are denoted by Fe(2)) and a strong distortion of octahedra in single layers (these positions are denoted by Fe(1)).

If the ratio between the numbers of double and single iron layers alternating in ferrihydrite is equal to 1 : 1, we find that the ratio between the occupancies of the Fe(2) and Fe(1) positions amounts to 2 : 1, which is usually observed in mineral ferrihydrites [7] and ferrihydrites of the organic origin [8].

Table 2. Mössbauer parameters of the dried biomass after thermal annealing

Annealing temperature, °C	IS ±0.005 mm/s	QS ±0.02 mm/s	W ±0.02 mm/s	S ±0.03	Position
20	0.395	0.49	0.35	0.45	Fe(2)
	0.388	0.88	0.33	0.36	Fe(1)
	0.377	1.25	0.35	0.19	Fe(3)
300	0.389	0.83	0.40	0.36	Fe(2)
	0.389	1.10	0.40	0.36	Fe(1)
	0.38	1.54	0.42	0.17	Fe(3)
	1.145	1.82	0.35	0.04	Fe^{2+}
	0.991	2.60	0.25	0.04	Fe^{2+}
	0.986	3.10	0.33	0.04	Fe^{2+}
400	0.374	0.51	0.31	0.10	Fe(2)
	0.371	0.84	0.40	0.38	Fe(1)
	0.358	1.26	0.41	0.37	Fe(3)
	0.352	1.73	0.40	0.13	Fe(3)
	1.30	2.21	0.20	0.02	Fe^{2+}
500	0.383	0.64	0.40	0.23	Fe(2)
	0.371	1.10	0.45	0.34	Fe(1)
	0.352	1.62	0.52	0.23	Fe(3)
	1.031	2.76	0.53	0.03	Fe^{2+}
700	0.395	0.64	0.49	0.45	Fe(2)
	0.392	1.12	0.38	0.24	Fe(1)
	0.416	1.63	0.28	0.13	Fe(3)
	0.367	−0.42	0.15−0.61	0.18	$\alpha\text{-}Fe_2O_3$

Note: IS is the isomer chemical shift with respect to α-Fe, QS is the quadrupole splitting, W is the line width, and S is the fractional occupancy of the position.

Now, we discuss the origin of the Fe(3) positions with a strong local distortion. When an iron cation passes from the occupied layer to the empty layer, it turns out to be in the octahedron shared by the face with the occupied octahedron of the neighboring layer. For example, it is known from the hematite structure [9] that, in the formation of a pair of face-shared octahedra, the iron cations tend to repel from each other and leave the centers of the octahedra. As a result of this displacement, the local symmetry of cations sharply decreases, which leads to the large observed quadrupole splitting. Therefore, it is reasonable to assume that Fe(3) positions are formed when iron passes to the interlayer positions. In this case, there arises a pair of occupied octahedra shared by the face and the iron atoms of this pair belong to Fe(3).

In the as-prepared samples, the ratio between the occupancies of the double and single iron layers deviates from a ratio of 2 : 1 toward equalizing the occupancies of these layers. Moreover, there are approximately 20% of iron occupying the Fe(3) interlayer positions. During heating to 400°C, the fraction of iron occupying the double layers of octahedra (Fe(2) positions) decreases and the fraction of iron occupying octahedra shared by the face (Fe(3) positions) increases. The fraction of iron occupying the single layers (Fe(1) positions) remains almost unchanged (Table 2). The isomer chemical shift decreases for all positions. Therefore, during heating of ferrihydrite, double iron layers decompose and iron passes to the interlayer positions, which results in the formation of octahedral or hematite-like positions shared by faces. Figure 4 shows the dependences of the occupancy of the Fe ion positions in ferrihydrite on the annealing temperature. The occupancy of the single layers Fe(1) does change significantly, because the increase in the number of single layers in the decomposition of double layers is compensated for by their decrease due to the formation of hematite-like positions. In X-ray powder diffraction analysis, the reflections of hematite were recorded for the samples annealed at temperatures above 500°C. This suggests that the nanoparticles formed at the annealing temperature $T = 500$°C are in the superparamagnetic state ($d < 18$ nm) and further
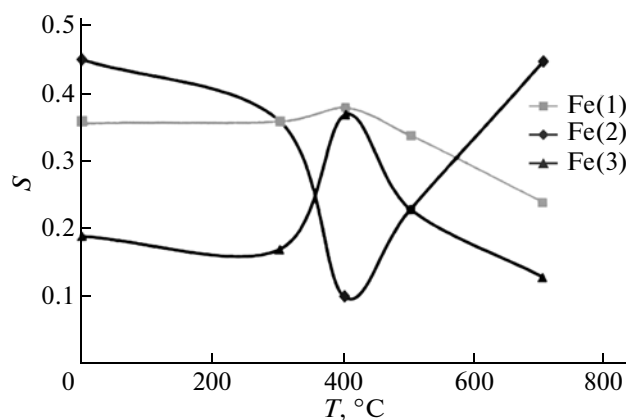
Fig. 4. Fractional occupancies of the Fe^{3+} ion positions in ferrihydrite as a function of the annealing temperature.

heat treatment leads to an increase in the sizes of hematite particles.

After heat treatment at 700°C, the Zeeman sextet appears in the Mössbauer spectrum and its hyperfine-structure parameters coincide with those for bulk hematite: IS = 0.367 mm/s, H = 507 kOe, and QS = −0.42 mm/s. The appearance of the Zeeman sextet in the spectrum at room temperature indicates that the material contains hematite crystals with sizes larger than 18 nm [10]. The occupancy of this phase is ~ 18% of the total iron content. In this case, the Fe(3) positions are recorded, and their fraction is 13%. Probably, these positions characterize the hematite nanoparticles in the superparamagnetic state; i.e., the hyperfine-structure parameters for the $Fe^{3+}(3)$ position can be considered characteristics of the nanosized super-paramagnetic state of hematite: IS = 0.34−0.36 mm/s and QS = 1.6−1.9 mm/s.

After annealing at T = 700°C, the Fe(2) and Fe(1) positions of iron ions are retained in the material. The ratio between the occupancies of these positions is 2 : 1, which is typical of ferrihydrites. Thus, as a result of heat treatment, ferrihydrite particles become more defective because of the increase in the number of Fe(3) positions, which are nuclei in the formation of the hematite phase. The complete transformation ferrihydrite ⟶ hematite does not take place. The final products of decomposition of defect ferrihydrite as a result of heat treatment is more "stoichiometric" ferrihydrite and the hematite phase.

4. CONCLUSIONS

Thus, the study of bacterial ferrihydrite has shown that *Klebsiella oxytoca* bacteria can accumulate iron in the composition of ferrihydrite consisting of double and single layers of iron ions. Cations of these layers Fe(1) and Fe(2) are located in coordination octahe-

dra, which are shared by edges with neighboring occupied octahedra. The Fe(3) positions should be considered defects in the ferrihydrite structure, because they are formed when iron passes to layers of empty octahedra. The octahedra of these positions, which are shared by faces with the octahedra of neighboring layers occupied by iron, become strongly distorted. Pairs of strongly distorted octahedra shared by the face are typical of the hematite structure, so that it is reasonable to treat the Fe(3) positions as hematite-like positions. The hyperfine-structure parameters for the Fe(3) position should be considered characteristics of the nanosized superparamagnetic hematite state: IS = 0.34−0.36 mm/s and QS = 1.6−1.9 mm/s.

REFERENCES

1. P. Tartaj, M. del Puerto Morales, S. Veintemillas-Verdaguer, T. Gonzalez-Carreno, and C. J. Serna, J. Phys. D: Appl. Phys. **36**, 182 (2003).

2. I. Oshtrakh, O. B. Milder, V. A. Semionkin, P. G. Prokopenko, A. B. Livshits, A. A. Kozlov, and A. I. Pikulev, Z. Naturforsch., A: Phys. Sci. **57**, 566 (2002).

3. Yu. L. Raikher, V. I. Stepanov, S. V. Stolyar, V. P. Ladygina, D. A. Balaev. L. A. Ishchenko, and M. Balasoiu, Fiz. Tverd. Tela (St. Petersburg) **52** (2), 277 (2010) [Phys. Solid State **52** (2), 298 (2010)].

4. F. V. Chukhrov, B. B. Zvyagina, A. I. Gorshkov, L. P. Ermilova, and V. V. Balashova, Izv. Akad. Nauk SSSR, Ser. Geol., No. 4, 23 (1973).

5. E. Jansen, A. Kyek, W. Schafer, and U. Schwertmann, Appl. Phys. **74**, 1004 (2002).

6. S. V. Stolyar, O. A. Bayukov, Yu. L. Gurevich, E. A. Denisova, R. S. Iskhakov, V. P. Ladygina, A. P. Puzyr', P. P. Pustoshilov, L. A. Chekanova, and M. A. Bitekhtina, Materialovedenie, No. 7, 34 (2006).

7. M. L. Wade, D. C. Agresti, and T. J. Wdowiak, J. Geophys. Res. **104**, 8489 (1999).

8. M. I. Oshtrakh, O. B. Milder, V. A. Semionkin, L. I. Malakheeva, and P. G. Prokopenko, J. Radioanal. Nucl. Chem. **3**, 671 (2006).

9. R. Z. Blacke, R. E. Hessevick, T. Zoltai, and L. W. Finger, Am. Mineral. **51**, 123 (1996).

10. I. P. Suzdalev, *Nanotechnology: Physical Chemistry of Nanoclusters, Nanostructures, and Nanomaterials* (KomKniga, Moscow, 2006) [in Russian].

Translated by E. Chernokozhin